GENUINELY NONLINEAR MODELS FOR CONVECTION-DOMINATED PROBLEMS *

TRAIAN ILIESCU †

Abstract. This paper introduces a general, nonlinear subgrid-scale (SGS) model, having bounded artificial viscosity, for the numerical simulation of convection-dominated problems. We also present a numerical comparison (error analysis and numerical experiments) between this model and the most common SGS model of Smagorinsky, which uses a p-Laplacian regularization. The numerical experiments for the 2-D convection-dominated convection-diffusion test problem show a clear improvement in solution quality for the new SGS model. This improvement is consistent with the bounded amount of artificial viscosity introduced by the new SGS model in the sharp transition regions.

Key words. subgrid-scale model, artificial viscosity, p-Laplacian

AMS subject classifications. Primary 65N30; Secondary 76M10

1. Introduction. One of the fundamental difficulties in the numerical study of convection-dominated problems is that considerable information can be contained in small scales, below the level of the finest mesh. To represent these effects on the larger scales, different methodologies have been used in practical calculations. These methodologies have been successfully analyzed and implemented in the linear case of convection-diffusion problems (the streamline-diffusion method is probably the most successful in this class). For nonlinear problems (e.g., the Navier-Stokes equations), one of the most common methodologies is to use various subgrid-scale (SGS) models (see, e.g., [16], for a survey of these models). However, very little rigorous mathematical analysis has been done validating the effects of these nonlinear SGS terms on the underlying continuum model and on the discretization ultimately employed.

The goal of this paper is twofold. First, we introduce a general, nonlinear SGS model, having bounded artificial viscosity. Then, we start a careful comparison of this new SGS model with the most common SGS model of Smagorinsky [19], which uses a p-Laplacian regularization. Specifically, we present the error analysis for the corresponding finite element method (FEM) discretizations of the two SGS models, as well as numerical experiments for the 2-D convection-dominated convection-diffusion test problem with homogeneous Dirichlet boundary conditions:

$$-\varepsilon\Delta u + \mathbf{b}\cdot\nabla u + cu = f \quad \text{in} \quad \Omega, \tag{1.1}$$

$$u = 0 \qquad\qquad\qquad\quad \text{on } \partial\Omega, \tag{1.2}$$

where Ω is a polyhedral domain in $\mathbb{R}^d$ (d = 2, 3), $\mathbf{b} : \Omega \to \mathbb{R}^d$, $c : \Omega \to \mathbb{R}$, $f : \Omega \to \mathbb{R}$, and $0 < \varepsilon \ll 1$. This test problem is a first and essential step in a careful numerical comparison of the two SGS models, in that there is little (if any) hope of understanding the effects of these SGS terms upon the discretization of more general, nonlinear problems (as the Navier-Stokes equations), without studying these effects on (1.1)–(1.2), first.

The most common approach for the discretization of the linear problem (1.1)–(1.2) is the streamline-diffusion finite element method (SDFEM). SDFEM, introduced by Hughes and Brooks [9], and mainly analyzed by Nävert [17] and Eriksson and Johnson [6], is a great improvement of the common upwind type methods and has been successfully implemented and tested on a wide variety of problems [10], [18]. SDFEM stabilizes (1.1)–(1.2) in a consistent way, introducing a linear amount of artificial viscosity (AV) in the direction of the flow, and reducing the need for extra stabilizing AV. Along these lines, a further way to

*This work was supported in part by the Mathematical, Information, and Computational Sciences Division subprogram of the Office of Advanced Scientific Computing Research, U.S. Dept. of Energy, under Contract W-31-109-Eng-38, and by NSF grants INT 9814115 and INT 9805563.

†Mathematics and Computer Science Division, Argonne National Laboratory, 9700 S. Cass Avenue, Argonne, IL 60439 (iliescu@mcs.anl.gov).

reduce the need for extra stabilizing AV is to apply the AV locally, via a Smagorinsky-type SGS term of the form

$$-\nabla \cdot (\mu h^{\sigma} \mid h\nabla u^h \mid^{p-2} \nabla u^h) \tag{1.3}$$

added to the discretization of the left-hand side (LHS) of (1.1). In the above formula, $|\cdot|$ is the Euclidian norm, h represents the meshwidth in the discretization of (1.1)–(1.2), u^h is the discretized solution, and μ, σ, and p are user-specified parameters. This extra nonlinear term introduces the AV in a selective way: it introduces a negligible amount of AV in smooth regions (where $|\nabla u^h|$ is small), and a stabilizing amount of AV in the sharp transition regions (where $\mid \nabla u^h \mid \sim O(h^{-1})$). The p-Laplacian AV term (1.3) stabilizes the discretization and also spreads the small (below the meshwidth) scales onto the computable mesh. This p-Laplacian AV term has been used in numerous challenging numerical applications; the Smagorinsky [19] model, which uses a p-Laplacian AV term, is one of the most popular models in the numerical simulation of turbulent flows. However, very little rigorous analysis, mathematical or numerical, has been done validating the corresponding continuum and discretized models (see [5], [4], [11]).

In Section 2, using the p-Laplacian's strong monotonicity, Minty's lemma [15], [13], and discrete inverse Sobolev's inequalities, we prove existence, uniqueness, max-norm stability, and a priori error estimates for u^h, the approximate solution of the discretization of (1.1)–(1.2) including the nonlinear AV term (1.3). This analysis follows the approach used by Layton in [11] and complements the one on the pure p-Laplacian problem [1], [2].

The p-Laplacian AV term (1.3), despite its well-known (see [11]) qualities, has the drawback of introducing an unbounded amount of AV in sharp transition regions, whereas just $O(h)$ AV is needed. Motivated by this drawback, we introduce in Section 3 a general, nonlinear, bounded AV term of the form

$$-\nabla \cdot (\mu h^{\sigma} a(\mid h\nabla u^h \mid)\nabla u^h) \tag{1.4}$$

added to the discretization of the LHS of (1.1). The parameters in (1.4) are the same as those in (1.3). The function $a(\cdot)$, however, instead of being a power function (and thus unbounded) as in the p-Laplacian AV term (1.3), is a general bounded, smooth, nonnegative, real-valued function, whose derivative is also bounded (see Figure 1.1).

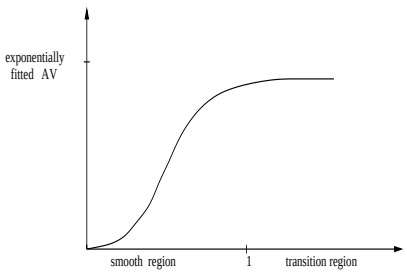

FIG. 1.1. *The graph of $a(\cdot)$; the horizontal axis represents $\mid h\nabla u^h \mid$.*

The nonlinear AV term (1.4) introduces a bounded amount of AV in the sharp transition regions, and almost no AV in the smooth regions.

Since the nonlinear bounded AV term (1.4) has no monotonicity properties, the error analysis for the corresponding model is much more challenging than the one for the p-Laplacian AV model. In Section 3, we prove existence, uniqueness, and a priori error estimates for u^h, the approximate solution of the discretization of (1.1)–(1.2) including the nonlinear AV term (1.4).

Numerical experiments reported in Section 4 show that, for problems exhibiting very sharp layers, the bounded AV model shows a visible improvement in solution quality versus the p-Laplacian AV model, while both can show a dramatic improvement over the common SDFEM method.

These numerical experiments, supported by a careful mathematical and numerical analysis, which we begin here, make the bounded nonlinear AV SGS model a promising approach for the numerical study of convection-dominated problems.

2. Error Analysis for the p-Laplacian AV Model. We begin by introducing the mathematical structures needed for the numerical analysis of the p-Laplacian AV model. Let $\Pi^h(\Omega)$ denote the finite element partition of Ω into face-to-face d-simplices (d=2,3) with meshwidth (maximum d-simplex diameter) h. The minimum angle in $\Pi^h(\Omega)$, θ_{min}, is assumed to be bounded away from zero uniformly in h. The norm $\|\cdot\|$ denotes the usual $L^2(\Omega)$ norm, and $\|\cdot\|_{L^p}$ denotes the $L^p(\Omega)$ norm. The norm on $W^{-1,q}$, the dual of the Sobolev space $W_0^{1,p}$, is defined by

$$||\Phi||_{W^{-1,q}} := \sup_{0\neq v\in W_0^{1,p}} \frac{(\Phi, v)}{||\nabla v||_{L^p}} ,$$

where $\frac{1}{p}+\frac{1}{q}=1$.

Let $X = H_0^1(\Omega)$, its norm $\|\cdot\|_X := \|\cdot\|_{1,\Omega}$, and $(\cdot,\cdot)$ the $L^2(\Omega)$ inner product. The usual weak formulation [7], [8], [10] of problem (1.1)–(1.2) is to find $u \in X$ satisfying

$$\varepsilon(\nabla u, \nabla v) + (\mathbf{b}\cdot\nabla u, v) + (cu, v) = (f, v) \qquad \forall v \in X \ . \tag{2.1}$$

We define an energy-norm associated with (2.1):

$$|||v||| := \left(\varepsilon||\nabla v||^2 + ||v||^2\right)^{1/2} \ .$$

The spaces X^h are associated conforming finite element spaces, $X^h \subset X$, and $B(\cdot,\cdot)$ represents the usual bilinear form associated with (2.1). Specifically, for $u, v \in X$

$$B(u,v) := \varepsilon(\nabla u, \nabla v) + (\mathbf{b}\cdot\nabla u, v) + (cu, v) \ . \tag{2.2}$$

Using the Riesz representation theorem, define $AV_p : W_0^{1,p} \to (W_0^{1,p})'$ by

$$(AV_p(u), v) := \mu h^\sigma (|\ h\nabla u\ |)^{p-2}\nabla u, \nabla v) \quad \forall u, v \in W_0^{1,p}, \tag{2.3}$$

with $\mu > 0,\ \sigma > 0,$ and $p \geq 2$.

Since $AV_p(\cdot)$ is associated with the p-Laplacian, its monotonicity properties are documented in many places (see, e.g., [15], [13]). We summarize them here:

$$(AV_p(u) - AV_p(v), u - v) \geq \mu C_1(p) h^{\sigma+p-2}\|\nabla(u-v)\|_{L^p}^p \tag{2.4}$$

$$\|AV_p(u) - AV_p(v)\|_{W^{-1,q}} \leq \mu C_2(p) h^{\sigma+p-2} r^{p-2}\|\nabla(u-v)\|_{L^p} \ , \tag{2.5}$$

where $C_1(p)$ and $C_2(p)$ are constants independent of h, $r := \max\{\|\nabla u\|_{L^p}, \|\nabla v\|_{L^p}\}$, and $\frac{1}{p}+\frac{1}{q}=1$.

By a coercivity argument [18], there exists a unique solution of (2.1), provided that there exists a constant $\tilde{\alpha}$ such that

$$\inf_{\mathbf{x}\in\Omega}\left\{c(\mathbf{x}) - \frac{1}{2}(\nabla\cdot\mathbf{b})(\mathbf{x})\right\} \geq \tilde{\alpha} \geq 0 \ . \tag{2.6}$$

We now begin the study of the p-Laplacian AV model for the convection-dominated convection-diffusion problem (1.1)–(1.2), given by

$$\mu h^{\sigma}(\mid h\nabla u^h \mid^{p-2} \nabla u^h, \nabla v) + \varepsilon(\nabla u^h, \nabla v) + (\mathbf{b}\cdot\nabla u^h, v) + (cu^h, v) = (f, v) \ , \quad \forall v \in X^h \ . \tag{2.7}$$

Since the above model is nonlinear, it is not altogether obvious that an approximate solution u^h exists. The following lemma answers this question.

LEMMA 2.1. *(Existence and uniqueness of u^h) There exists a unique solution for (2.7).*

Proof. The proof follows from the coercivity of the bilinear form in (2.7), the strong monotonicity (2.4) of the p-Laplacian AV term, and Minty's lemma [15], [13]. □

For the error analysis we will need to use discrete tools linking the $L^2(\Omega)$ and $L^p(\Omega)$ norms. In particular, most commonly used finite element spaces satisfy the following inverse inequality and Poincaré inequality :

$$C_1 h\|\nabla v\| \le \|v\| \le C_2\|\nabla v\| \ , \quad \forall v \in X^h, \tag{2.8}$$

where C_1, C_2 are constants independent of h.

We will also need the following $L^p - L^2$ -type inverse inequality [[11], Lemma 2.1]:

LEMMA 2.2. *Let θ_{min} be the minimum angle in the triangulation and $M^k = \{v(x) : v \in C(\bar{\Omega}), v \mid_T \in P_k(T)\ \forall T \in \Pi^h(\Omega)\}$, P_k being the polynomials of degree $\le k$. Then, there is a $C = C(\theta_{min}, p, k)$ such that for $2 \le p < \infty$, $d = 2, 3$, and all $v \in M^k$*

$$\|\nabla v\|_{L^p(\Omega)} \le C h^{\frac{d}{2}(\frac{2-p}{p})}\|\nabla v\|. \tag{2.9}$$

A stability result of method (2.7) with p-Laplacian regularization is given by the following lemma.

LEMMA 2.3. *If $p > d$, then*

$$\|u^h\| \le \frac{\|f\|}{C\varepsilon + \tilde{\alpha}}, \quad \textit{and} \tag{2.10}$$

$$\|u^h\|_{L^\infty} \le C h^{-\frac{\sigma+p-2}{p-1}}\|f\|_{W^{-1,q}}^{\frac{1}{p-1}}, \tag{2.11}$$

where C is a generic constant independent of h.

Proof. Setting $v = u^h$ in (2.7), we get

$$\mu h^{\sigma+p-2}\|\nabla u^h\|_{L^p}^p + B(u^h, u^h) = (f, u^h) \ .$$

Using (2.6), (2.8), the above equality, and Hölder's inequality, we get

$$(C_2^{-2}\varepsilon + \tilde{\alpha})\|u^h\|^2 \le \|f\|\|u^h\|, \quad \text{and}$$
$$\mu h^{\sigma+p-2}\|\nabla u^h\|_{L^p}^p \le \|f\|_{W^{-1,q}}\|\nabla u^h\|_{L^p},$$

where $\frac{1}{p} + \frac{1}{q} = 1$. Therefore,

$$\|u^h\| \le \frac{\|f\|}{C_2^{-2}\varepsilon + \tilde{\alpha}} \quad ,$$

which proves (2.10), and

$$\mu h^{\sigma+p-2}\|\nabla u^h\|_{L^p}^{p-1} \le \|f\|_{W^{-1,q}} \ ,$$

which implies

$$\|\nabla u^h\|_{L^p} \leq \mu^{-\frac{1}{p-1}} h^{-\frac{\sigma+p-2}{p-1}} \|f\|^{\frac{1}{p-1}}_{W^{-1,q}} .$$

By the Sobolev embedding theorem, we have that, for $p > d$,

$$\|u^h\|_{L^\infty} < C(\Omega)\|\nabla u^h\|_{L^p}.$$

From the above two inequalities, (2.11) now follows. □

2.1. A Priori Error Analysis. An a priori error estimate for method (2.7) is given by the following theorem.

THEOREM 2.4. *Suppose that X^h satisfies estimate (2.9) and that $\inf_{w\in X^h} ||\nabla w||_{L^p} \leq C||\nabla u||$. Then,*

$$\begin{aligned}
&\mu C h^{\sigma+p-2}\|\nabla(u-u^h)\|^p_{L^p} + \varepsilon\|\nabla(u-u^h)\|^2 + \|u-u^h\|^2 \leq \\
&C \inf_{w\in X^h} \{ \quad \|u-w\|^2 + \varepsilon\|\nabla(u-w)\|^2 + \|\nabla(u-w)\|^2 + \mu h^{\sigma+p-2}\|\nabla(u-w)\|^p_{L^p} + \\
&\mu^2\varepsilon^{-1}h^{2\sigma+2(p-2)+d(\frac{2-p}{p})}\|\nabla(u-w)\|^2_{L^p}||\nabla u||^{2(p-2)}_{L^p} \quad \} + \mu^2 C\varepsilon^{-1}h^{2\sigma+2(p-2)+d(\frac{2-p}{p})}\|\nabla u\|^{2p-2}_{L^p},
\end{aligned}$$

where C is a generic constant independent of h.

Proof. The error bound is proven by using Galerkin orthogonality and the monotonicity of $AV_p(\cdot)$ (2.4). First, the error equation is derived. Subtracting (2.7) from (2.1), we get

$$-(AV_p(u^h), v) + B(e, v) = 0 \quad \forall v \in X^h, \tag{2.12}$$

where $e = u - u^h$. Let $w \in X^h$ be arbitrary and define $\phi = w - u^h \in X^h$, $\eta = u - w$ (note that $e = \eta + \phi$). Adding and subtracting terms as appropriate and using the bilinearity of $B(\cdot,\cdot)$, we get

$$\begin{aligned}
(AV_p(w), v) - (AV_p(u^h), v) + B(\phi, v) = (AV_p(w), v) - (AV_p(u), v) \\
- B(\eta, v) + (AV_p(u), v) \quad \forall v \in X^h \ .
\end{aligned} \tag{2.13}$$

Using (2.5), we also have

$$\begin{aligned}
(AV_p(u), v) &= (AV_p(u), v) - (AV_p(0), v) \\
&\leq \|AV_p(u) - AV_p(0)\|_{W^{-1,2}}\|\nabla v\| \\
&\leq \mu C_2(p) h^{\sigma+p-2}\|\nabla u\|^{p-1}_{L^p}\|\nabla v\| \ .
\end{aligned} \tag{2.14}$$

If we set $v = \phi$ (since $\phi \in X^h$) and use the strong monotonicity of $AV_p(\cdot)$ (2.4) and the coercivity of $B(\cdot,\cdot)$ on the LHS of (2.13), the local-Lipschitz continuity of $AV_p(\cdot)$ (2.5) and the continuity of $B(\cdot,\cdot)$ on the right-hand side (RHS), and (2.14), we obtain

$$\begin{aligned}
\mu C_1(p) h^{\sigma+p-2}\|\nabla\phi\|^p_{L^p} + \varepsilon\|\nabla\phi\|^2 + \tilde{\alpha}\|\phi\|^2 \leq \mu C_2(p) h^{\sigma+p-2} r^{p-2}\|\nabla\phi\|_{L^p}\|\nabla\eta\|_{L^p} + \varepsilon\|\nabla\eta\|\|\nabla\phi\| \\
+ K_1\|\nabla\eta\|\|\phi\| + K_2\|\eta\|\|\phi\| \\
+ \mu C_2(p) h^{\sigma+p-2}\|\nabla u\|^{p-1}_{L^p}\|\nabla\phi\|_{L^p},
\end{aligned}$$

where $r = \max\{\|\nabla u\|_{L^p}, \|\nabla w\|_{L^p}\}$.
Using Lemma 2.2 and the Cauchy-Schwarz inequality on the RHS yields

$$\begin{aligned}
\mu h^{\sigma+p-2} C_1(p)\|\nabla\phi\|^p_{L^p} + C\varepsilon\|\nabla\phi\|^2 + C\|\phi\|^2 \leq \mu^2 C(p)\varepsilon^{-1} r^{2(p-2)} h^{2\sigma+2(p-2)+d(\frac{2-p}{p})}\|\nabla\eta\|^2_{L^p} \\
+ \mu^2 C(p)\varepsilon^{-1} h^{2\sigma+2(p-2)+d(\frac{2-p}{p})}\|\nabla u\|^{2p-2}_{L^p} \\
+ C\varepsilon\|\nabla\eta\|^2 + C\|\nabla\eta\|^2 \ .
\end{aligned}$$

Since $\|u_1+u_2\|_{L^p}^p \le C(p)(\|u_1\|_{L^p}^p + \|u_2\|_{L^p}^p)$, and $r \le C\|\nabla u\|_{L^p}$ at infimum, the result now follows taking the infimum over $w \in X^h$ of the above inequality and using the triangle inequality. ∎

REMARK 2.1. *L^p stability of the L^2 projection into finite element spaces is proven in [3].*

REMARK 2.2. *Theorem 2.4 also proves the convergence of u^h. Indeed, since $\sigma > 0$, $p \ge 2$, and $d = 2, 3$, we get $2\sigma + 2(p-2) + \frac{d(d-p)}{p} > 0$.*

REMARK 2.3. *The convergence of u^h is not uniform in ε. However, for many practical choices of the parameters σ and p, the scaling between ε and h is reasonable. For example, in 2-D ($d = 2$), for $p \ge 3$ and $\sigma \ge 1$, we have $2\sigma + (p-2)\left(2 - \frac{2}{p}\right) \ge \frac{10}{3}$, and thus $\varepsilon > O(h^{\frac{10}{3}})$ in order to get convergence of u^h. In 3-D ($d = 3$), for $p \ge 3$ and $\sigma \ge 1$, we have $2\sigma + (p-2)\left(2 - \frac{2}{p}\right) \ge 3$, and thus $\varepsilon > O(h^3)$ in order to get convergence of u^h.*

3. Error Analysis for the General Bounded AV Model. In this section we study the general, bounded AV model used for the discretization of the convection-dominated convection-diffusion problem (1.1)–(1.2):

$$\mu h^\sigma (a(|\ h\nabla u^h\ |)\nabla u^h, \nabla v) + \varepsilon(\nabla u^h, \nabla v) + (\mathbf{b}\cdot\nabla u^h, v) + (cu^h, v) = (f, v)\ , \quad \forall v \in X^h, \tag{3.1}$$

We start with a very general AV model (i.e. a very general function $a(\cdot)$), and then we impose restrictions on it in order to obtain existence, uniqueness, and convergence for the solution of the discretized problem. In particular, we prove an a priori error bound for u^h, the approximate solution of (3.1).

Here $\sigma > 0$ and $\mu > 0$ are parameters to be determined, and $a(\cdot)$ is a smooth, bounded, nonnegative function whose graph looks like that in Figure 1.1.

The shape of $a(\cdot)$ makes the AV term $\mu h^\sigma (a(|\ h\nabla u^h\ |)\nabla u^h, \nabla v)$ fit the description we gave in the introduction: the amount of AV introduced in the discretization (3.1) is negligible in the smooth regions (where the gradient is small) and bounded where the gradient is large:

$$\mu h^\sigma (|\ h\nabla u^h\ |^{p-2}\ \nabla u^h, \nabla v) \sim \begin{cases} h^\sigma(\nabla u^h, \nabla v)\ , & \text{where } |\ \nabla u^h\ | \sim O(h^{-1})\ , \\ h^{p+\sigma-2}(\nabla u^h, \nabla v)\ , & \text{where } |\ \nabla u^h\ | \sim O(1)\ . \end{cases}$$

We now seek conditions upon $a(\cdot)$ and μ, sufficient for the existence, uniqueness, and convergence of u^h.

LEMMA 3.1. *(Existence of u^h) Assume that $\mathbf{b}(\cdot)$ and $c(\cdot)$ are smooth enough functions and that (2.6) is satisfied.*

Then, provided $a(\cdot) \ge 0$, there exists a solution to (3.1), and we have the following a priori bound:

$$\|u^h\|_1 \le C(f, \varepsilon, h) := \frac{\|f\|_{-1}}{\frac{\varepsilon}{1+C_2^2} + \frac{\tilde{\alpha}}{1+C_1^{-2}h^{-2}}}\ , \tag{3.2}$$

where C_1, C_2 are constants independent of h.

REMARK 3.1. *Condition (2.6) is a common condition that ensures existence and uniqueness of u, the solution of the continuous problem (2.1).*

Proof. Since $\dim(X^h) < \infty$, existence will follow from Schauder's fixed point theorem once we have proven an a priori bound on any *possible* solution u^h.

Using (2.8), we get

$$\|\nabla u^h\|^2 \ge \frac{\|u^h\|_1^2}{1+C_2^2} \quad \text{and} \quad \|u^h\|^2 \ge \frac{\|u^h\|_1^2}{1+C_1^{-2}h^{-2}}, \tag{3.3}$$

where C_1, C_2 are constants independent of h.

Letting $v = u^h$ in (3.1) yields

$$\mu h^\sigma (a(\mid h\nabla u^h \mid)\nabla u^h, \nabla u^h) + \varepsilon(\nabla u^h, \nabla u^h) + (\mathbf{b}\cdot\nabla u^h, u^h) + (cu^h, u^h) = (f, u^h) \ . \tag{3.4}$$

Since $a(\cdot)$ is nonnegative and $\mu > 0$, we have

$$\mu h^\sigma (a(\mid h\nabla u^h \mid)\nabla u^h, \nabla u^h) \geq 0 \ .$$

Integrating by parts, using (2.6) and the above inequality on the LHS, and the Cauchy-Schwarz inequality on the RHS of (3.4), we have

$$\varepsilon\|\nabla u^h\|^2 + \tilde{\alpha}\|u^h\|^2 \leq \|f\|_{-1}\|u^h\|_1 \ .$$

Using (3.3) in the above inequality, we get

$$\left(\frac{\varepsilon}{1+C_2^2} + \frac{\tilde{\alpha}}{1+C_1^{-2}h^{-2}}\right)\|u^h\|_1^2 \leq \|f\|_{-1}\|u^h\|_1,$$

which yields (3.2). Estimate (3.2) and Schauder's fixed point theorem prove existence of u^h, the solution to (3.1). □

REMARK 3.2. *Notice that for the existence of u^h, we did not impose any new conditions on $a(\cdot)$ (other than those already imposed in the beginning of the section) or on μ. Thus, any function $a(\cdot)$ whose graph resembles the one in Figure 1.1 is admissible.*

The following proposition proves the uniqueness of u^h, with a very general condition on $a(\cdot)$. Note that usually the uniqueness is proven by means of monotonicity arguments. These arguments fail in this case, and we have to use nontrivial nonlinear variational analysis arguments [13] instead.

LEMMA 3.2. *(Uniqueness of u^h) Assume that the conditions in Lemma 2.2 are satisfied and that*

$$a'(x) \geq 0 \ , \quad \forall x \geq 0. \tag{3.5}$$

Then, there exists a unique solution u^h to (3.1).

Proof. Assume there are two solutions u_1^h, u_2^h in X^h. Subtracting the two corresponding equations, we get

$$\begin{aligned}\mu h^\sigma (a(\mid h\nabla u_1^h \mid)\nabla u_1^h - a(\mid h\nabla u_2^h \mid)\nabla u_2^h, \nabla v) + \varepsilon(\nabla u_1^h - \nabla u_2^h, \nabla v)\\ +(\mathbf{b}\cdot\nabla u_1^h - \mathbf{b}\cdot\nabla u_2^h, v) + (cu_1^h - cu_2^h, v) = 0 \quad \forall v \in X^h \ .\end{aligned}$$

Letting $v := u_1^h - u_2^h \in X^h$, integrating by parts, and using (2.6) in the above equation, we have

$$\begin{aligned}\mu h^\sigma (a(\mid h\nabla u_1^h \mid)\nabla u_1^h - a(\mid h\nabla u_2^h \mid)\nabla u_2^h, \nabla(u_1^h - u_2^h))\\ +\varepsilon\|\nabla(u_1^h - u_2^h)\|^2 + \tilde{\alpha}\|(u_1^h - u_2^h)\|^2 \leq 0\end{aligned} \tag{3.6}$$

The first term in the above inequality can be rewritten as

$$\frac{\mu h^\sigma}{h^2}(a(\mid h\nabla u_1^h \mid)h\nabla u_1^h - a(\mid h\nabla u_2^h \mid)h\nabla u_2^h, h\nabla(u_1^h - u_2^h)) \ . \tag{3.7}$$

Consider now the following functional:

$$\begin{aligned} I &: H^1(\Omega) \to \mathbb{R} \\ I(U) &:= \int_\Omega A(\mid \nabla U(\mathbf{x}) \mid)d\mathbf{x} \ ,\end{aligned}$$

where

$$A : [0,\infty) \to \mathbb{R}$$
$$A(x) = \int_0^x t a(t) dt \ .$$

Notice that

$$\begin{aligned} dI(U,V) &= \int_\Omega A'(\mid \nabla U \mid) \frac{\nabla U}{\mid \nabla U \mid} \cdot \nabla V \, d\mathbf{x} \\ &= \int_\Omega a(\mid \nabla U \mid) \nabla U \cdot \nabla V \, d\mathbf{x}, \end{aligned}$$

where $dI(U,V)$ is the Gâteaux derivative of I at U in the direction V.
Letting $U_1 := hu_1, U_2 := hu_2$, and $V := U_1 - U_2$, (3.7) reads

$$\frac{\mu h^\sigma}{h^2} \left(dI(U_1, V) - dI(U_2, V) \right) \ ,$$

which, by the Fundamental Theorem of Calculus, is equal to

$$\begin{aligned} &\frac{\mu h^\sigma}{h^2} \int_0^1 \frac{d}{dt} dI(U_2 + t(U_1 - U_2), V) dt \\ &= \frac{\mu h^\sigma}{h^2} \int_0^1 \frac{d}{dt} \int_\Omega a(\mid \nabla (U_2 + t(U_1 - U_2)) \mid) \nabla (U_2 + t(U_1 - U_2)) \cdot \nabla V \, d\mathbf{x} dt \\ &= \frac{\mu h^\sigma}{h^2} \int_0^1 \int_\Omega a'(\mid \nabla (U_2 + t(U_1 - U_2)) \mid) \frac{\nabla (U_2 + t(U_1 - U_2)) \cdot \nabla V}{\mid \nabla (U_2 + t(U_1 - U_2)) \mid} \nabla (U_2 + t(U_1 - U_2)) \cdot \nabla V \\ &+ a(\mid \nabla (U_2 + t(U_1 - U_2)) \mid) \mid \nabla V \mid^2 d\mathbf{x} dt \end{aligned}$$

Since $a'(x) \geq 0 \quad \forall x \geq 0$ by (3.5), and $a(x) \geq 0 \quad \forall x \geq 0$, the above expression is nonnegative. Thus, (3.7) is nonnegative; nonnegativity of (3.7) and (3.6) imply

$$\varepsilon \|\nabla (u_1^h - u_2^h)\|^2 + \tilde{\alpha} \|(u_1^h - u_2^h)\|^2 \leq 0 \ .$$

Therefore, since $\varepsilon > 0, \tilde{\alpha} \geq 0$, and $u_1^h - u_2^h \in X^h \subseteq H_0^1(\Omega)$, we get

$$u_1^h = u_2^h .$$

□

REMARK 3.3. *Note that condition (3.5) is satisfied by any function $a(\cdot)$ whose graph resembles the one in Figure 1.1.*

3.1. A Priori Error Analysis. In this subsection we present the a priori error analysis for the approximate solution u^h. For a very general function $a(\cdot)$, this a priori error analysis is summarized in the following theorem:

THEOREM 3.3. *Assume that $a(\cdot)$ is a positive, increasing function and that $\mathbf{b}(\cdot)$ and $c(\cdot)$ are continuous on $\bar{\Omega}$. Further suppose*

$$a(x) \leq 1 \ , \quad \forall x \geq 0 \ . \tag{3.8}$$

Then, we have the following a priori estimate:

$$\frac{\varepsilon}{8}\|\nabla(u-u^h)\|^2+\frac{\tilde{\alpha}}{4}\|(u-u^h)\|^2 \leq \inf_{w\in X^h}\left\{\left(\frac{3\varepsilon}{4}+\frac{K_1}{\tilde{\alpha}}\right)\|\nabla(w-u)\|^2+\left(\frac{K_2}{\tilde{\alpha}}+\frac{\tilde{\alpha}}{2}\right)\|w-u\|^2\right\}+ \frac{1}{\varepsilon}\left(\frac{\mu h^\sigma||f||_{-1}}{\varepsilon+\tilde{\alpha}C_1^2h^2}\right)^2,$$

where C_1, C_2, K_1, K_2 are constants independent of h, and $\tilde{\alpha}$ is the constant given by (2.6).

Proof. Subtracting (3.1) from (2.1), and using the fact that $X^h \subseteq X$, we get

$$-\mu h^\sigma(a(|\ h\nabla u^h\ |)\nabla u^h,\nabla v)+\varepsilon(\nabla(u-u^h),\nabla v)+(\mathbf{b}\cdot\nabla(u-u^h)+c(u-u^h),v)=0\ , \qquad \forall v\in X^h.$$

Let $w\in X^h$. Set $e := u-u^h$, $\eta = w-u$, $\varphi = w-u^h \in X^h$, and notice that $e=\varphi-\eta$. Therefore, the above equation reads

$$\varepsilon(\nabla\varphi,\nabla v)+(\mathbf{b}\cdot\nabla\varphi+c\varphi,v)=\varepsilon(\nabla\eta,\nabla v)+(\mathbf{b}\cdot\nabla\eta+c\eta,v)+\mu h^\sigma(a(h\mid\nabla u^h\mid)\nabla u^h,\nabla v)\ .$$

Setting $v=\varphi$ yields

$$\varepsilon\|\nabla\varphi\|^2+(\mathbf{b}\cdot\nabla\varphi+c\varphi,\varphi)=\varepsilon(\nabla\eta,\nabla\varphi)+(\mathbf{b}\cdot\nabla\eta+c\eta,\varphi)+\mu h^\sigma(a(|\ h\nabla u^h\ |)\nabla u^h,\nabla\varphi)\ .$$

Integrating by parts and using (2.6) on the LHS, and the Cauchy Schwarz inequality on the RHS, we have

$$\begin{aligned}\varepsilon\|\nabla\varphi\|^2+\tilde{\alpha}\|\varphi\|^2 \leq{}& \frac{\varepsilon}{2}\|\nabla\eta\|^2+\frac{\varepsilon}{2}\|\nabla\varphi\|^2+\frac{1}{\tilde{\alpha}}\|\mathbf{b}\cdot\nabla\eta\|^2+\frac{\tilde{\alpha}}{4}\|\varphi\|^2+\frac{1}{\tilde{\alpha}}\|c\eta\|^2+\frac{\tilde{\alpha}}{4}\|\varphi\|^2\\ &+\frac{1}{\varepsilon}(\mu^2h^{2\sigma}a(|\ h\nabla u^h\ |)\|\nabla u^h\|^2+\frac{\varepsilon}{4}\|\nabla\varphi\|^2\end{aligned}$$

Notice that the functions $\mathbf{b}(\cdot)$ and $c(\cdot)$ are continuous on $\bar{\Omega}$ (by hypothesis) and therefore bounded. Using this remark and (3.8), we have

$$\begin{aligned}\varepsilon\|\nabla\varphi\|^2+\tilde{\alpha}\|\varphi\|^2 \leq{}& \frac{\varepsilon}{2}\|\nabla\eta\|^2+\frac{\varepsilon}{2}\|\nabla\varphi\|^2+\frac{K_1}{\tilde{\alpha}}\|\nabla\eta\|^2+\frac{\tilde{\alpha}}{4}\|\varphi\|^2+\frac{K_2}{\tilde{\alpha}}\|\eta\|^2+\frac{\tilde{\alpha}}{4}\|\varphi\|^2\\ &+\frac{1}{\varepsilon}\mu^2h^{2\sigma}\|\nabla u^h\|^2+\frac{\varepsilon}{4}\|\nabla\varphi\|^2,\end{aligned}\tag{3.9}$$

where K_1, K_2 are constants independent of h. Using (2.8) and (3.5) yields

$$\|\nabla u^h\| \leq \frac{\|f\|_{-1}}{\varepsilon+\tilde{\alpha}C_1^2h^2}\ .$$

Thus, (3.9) becomes

$$\frac{\varepsilon}{4}\|\nabla\varphi\|^2+\frac{\tilde{\alpha}}{2}\|\varphi\|^2 \leq \frac{\varepsilon}{2}\|\nabla\eta\|^2+\frac{K_1}{\tilde{\alpha}}\|\nabla\eta\|^2+\frac{K_2}{\tilde{\alpha}}\|\eta\|^2+\frac{1}{\varepsilon}\left(\frac{\mu h^\sigma||f||_{-1}}{\varepsilon+\tilde{\alpha}C_1^2h^2}\right)^2\ .$$

By the triangle inequality, we get

$$\frac{1}{2}\left(\frac{\varepsilon}{4}\|\nabla(\varphi-\eta)\|^2+\frac{\tilde{\alpha}}{2}\|(\varphi-\eta)\|^2\right) \leq \frac{3\varepsilon}{4}\|\nabla\eta\|^2+\frac{K_1}{\tilde{\alpha}}\|\nabla\eta\|^2+\left(\frac{K_2}{\tilde{\alpha}}+\frac{\tilde{\alpha}}{2}\right)\|\eta\|^2+\frac{1}{\varepsilon}\left(\frac{\mu h^\sigma||f||_{-1}}{\varepsilon+\tilde{\alpha}C_1^2h^2}\right)^2\ .$$

Notice that $e = \varphi - \eta = u - u^h$ does not depend on w; thus, taking the infimum on w of both sides of the above inequality, proves the theorem. □

REMARK 3.4. *The* a priori *error estimate in Theorem 3.3 gives convergence of the approximate solution u^h to the exact solution u. The convergence is not uniform in ε. However, by choosing $a(\cdot)$ suitably, the discretization can be made to be exponentially fitted in all transition regions. Thus, an attempt to prove uniform in ε convergence would be legitimate in this case.*

REMARK 3.5. *The inequality (3.8) is satisfied by any function whose graph resembles the one in Figure 1.1, and allows us to introduce only $O(h^\sigma)$ AV in the sharp transition regions.*

Summarizing the results in this section, for any parameters $\mu \geq 0$ and $\sigma \geq 0$, and for any smooth function $a(\cdot)$ satisfying

$$0 \leq a(x) \leq 1 \quad \forall x \geq 0$$
$$0 \leq a'(x) \quad \forall x \geq 0,$$

we proved existence, uniqueness, and convergence for the solution u^h of (3.1). Notice that, although our results hold true for a more general function $a(\cdot)$ satisfying the above relations, in practice we use a function whose graph resembles the one in Figure 1.1, introducing a negligible amount of AV in the smooth regions, and only $O(h^\sigma)$ in the sharp transition regions.

4. Numerical Experiments. In this section we present numerical tests for the SDFEM method, the p-Laplacian AV SGS method, and the bounded AV SGS method. All three methods are applied to two challenging problems with sharp layers. These problems are catastrophically structurally unstable (small perturbations in the data result in dramatic unphysical oscillations, overshooting, and undershooting in the approximate solution), a characteristic feature of more general nonlinear flows (e.g., turbulent flows).

The boundary value problem (1.1)–(1.2) is solved on the unit square $\Omega = (0,1) \times (0,1)$ by using a finite element discretization with conforming piecewise linears on a uniform mesh of isosceles right-angled triangles, with meshwidth h. However, the same qualitative results have been obtained when using conforming piecewise quadratics. The nonlinear problems (2.7) and (3.1) were solved by using a Picard-type iterative process (at each iteration we lagged the nonlinear term). All the matrices and the corresponding right-hand sides were assembled by using a second-order quadrature rule, and the resulting linear systems were solved by using the conjugate gradient squared (CGS) method [14].

Example 1. This problem is a slight modification of the one used as a benchmark in a study of nonconforming SDFEM [10] and has as the exact solution a circular blob (see Figure 4.1) with extremely sharp layers. We made the following parameter choices in (1.1)–(1.2): $\varepsilon = 10^{-3}$, $\mathbf{b} = (3,2)$, $c = 2$. The right-hand side and the boundary conditions were chosen such that

$$u(x,y) = \frac{1}{2} + \frac{\arctan[1000(r_0^2 - (x-x_0)^2 - (y-y_0)^2)]}{\pi},$$

with $x_0 = y_0 = 0.5$ and $r_0 = 0.25$, be the exact solution of (1.1)–(1.2). Note that, even though our analysis considers the homogeneous problem (1.1)–(1.2), the same analysis carries over in a straightforward way to the nonhomogeneous case.

First, we apply the usual SDFEM method to problem (1.1)–(1.2) [18]:

$$\varepsilon(\nabla u^h, \nabla v) + (\mathbf{b}\cdot\nabla u^h, v) + (cu^h, v) + \sum_{T\in\Pi^h} \delta(-\varepsilon\Delta u^h + \mathbf{b}\cdot\nabla u^h + cu^h, \mathbf{b}\cdot\nabla v)_T = \tag{4.1}$$
$$(f,v) + \sum_{T\in\Pi^h} \delta(f, \mathbf{b}\cdot\nabla v)_T, \qquad \forall v \in X^h,$$

where δ is a user-specified parameter. In our calculations, we used $\delta = h$, which is probably the most popular choice in SDFEM. Note also that, when using conforming linears, the Laplacian term Δu^h on the LHS of the above relation is zero on each element T.

The graph (surface plot and contour lines) of the corresponding approximation u^h is given in Figure 4.2. Note the poor solution quality: dramatic overshooting and undershooting, especially in the direction of the flow.

Next, we apply the p-Laplacian AV SGS method (2.7) to (1.1)–(1.2). Here, we used the following values for the user-specified parameters: $\mu = 10,\ \sigma = 1,\ p = 3$. The graph (surface plot and contour lines) of the corresponding approximation u^h is given in Figure 4.3. As expected, the approximate solution given by the p-Laplacian AV model is more accurate than the one given by the SDFEM method, since the former introduces a nonnegligible amount of AV only in the sharp transition layers, whereas the latter introduces the same amount of AV everywhere. Specifically, the fact that the p-Laplacian AV model introduces AV in a selective way (only in the sharp transition regions) is reflected in a dramatic reduction of the amount of overshooting and undershooting and in a visible improvement in solution quality.

The last model tested is the general, bounded AV SGS model (3.1). For the user-specified parameters we made the following choices: $\mu = 1,\ \sigma = 1,\ a(t) = -0.001 + 1/(1 + 999 \cdot e^{-100 \cdot t})$. The choice of $a(\cdot)$ needs explanation. As mentioned at the end of Section 3, an "admissible" function $a(\cdot)$ should resemble the "S-shaped" graph in Figure 1.1 and should also introduce a nonnegligible amount of AV only where $| \nabla u^h | \sim O(h^{-1})$. Thus, the user has to decide when exactly the gradient is "large," that is, for what value of $|h \nabla u^h|$ the value of $a(\cdot)$ should become nonnegligible. For this test problem, our choice was motivated by the parameter choice for the p-Laplacian AV term. For clarity, for the above parameter choices, we present in Figure 4.4 the graph of $a(\cdot)$ against the graph of the corresponding term in the p-Laplacian AV term (i.e., $10 \cdot |h \nabla u^h|$).

The graph (surface plot and contour lines) of the approximation u^h of the general, bounded AV model (3.1) is given in Figure 4.5. The solution quality is better than the one in Figure 4.3, in that the amount of overshooting and undershooting is visibly decreased, whereas the contour lines are much tighter. This increased sharpness of the layers is more obvious if we count the number of elements inside the layer in the surface plots: roughly two elements for the exact solution (Figure 4.1), four elements for the p-Laplacian AV SGS model (Figure 4.3), and two elements for the bounded AV SGS model (Figure 4.5). This improvement is due to the bounded amount of AV introduced by (3.1) in the sharp transition regions, just enough to spread the small scales on the resolvable mesh.

Since we know the exact solution, we can make more precise the above discussion and calculate the norm of the error in the three discretizations. In Table 4.1, for different meshwidths ($h = 1/16,\ h = 1/32,\ h = 1/64,\ h = 1/128$), we present the L^2-norm of the error (denoted by $||\mathrm{E}||_{L^2}$), the energy-norm of the error (denoted by $|||\mathrm{E}|||$), the l^2-norm of the undershoots (denoted by $||\mathrm{U}||_{l^2}$), and the l^2-norm of the overshoots (denoted by $||\mathrm{O}||_{l^2}$). Here, the overshoots are considered the values larger than one and are calculated as the difference from one, and the undershoots are considered the values less than zero and are calculated as the difference from zero.

The most important piece of information in Table 4.1 is that the L^2-norm of the error for the two nonlinear AV models is consistently better (except for $h = 1/16$, when the mesh is too coarse) than the corresponding error for the SDFEM. This improvement is quite dramatic as we refine the mesh: for $h = 1/128$, the L^2-norm of the error is decreased by three and four times, respectively. We have the same dramatic improvement (one order of magnitude) in the l^2-norm of the undershoots. The l^2-norm of the overshoots and the energy-norm of the error are also better for the two nonlinear AV models, even though not as dramatic.

Comparing the two nonlinear AV models, we see that the bounded AV model is consistently better. The most dramatic improvement is in the L^2-norm of the error (roughly, by 35%).

Example 2. This problem, known as the "skew-step" problem, is a slight modification of the benchmark

used in [12] for the study of oscillation absorption FEM. It has steep internal and boundary layers, which make it numerically unstable. In (1.1)–(1.2), we made the following parameter choices: $\varepsilon = 10^{-3}$, $\mathbf{b}(x,y) = (\cos\theta(1-\cos\theta\ x), \sin\theta(1-\sin\theta\ y))$, $\theta = 0.8$, $c = 0$, $f = 0$. The homogeneous boundary conditions (1.2) were changed to $u(x,y) = g(x,y)$ on $\partial\Omega$, where $g(x,y) = 1$, if $12y - 5x \geq 0.3$, $g(x,y) = 0$ otherwise. Note that $\nabla \cdot \mathbf{b} = -1$, so that condition (2.6) is satisfied.

First, as in Example 1, we apply the usual SDFEM method (4.1) to (1.1)–(1.2), with $\delta = h$. Next, we apply the p-Laplacian AV SGS method (2.7) to (1.1)–(1.2), with $\mu = 0.1$, $\sigma = 1$, $p = 3$. Finally, we apply the bounded AV SGS model (3.1), with $\mu = 0.3$, $\sigma = 1$, $a(t) = -0.02 + 1/(1 + 49 \cdot e^{-5.7 \cdot t})$. The parameter choices for the two nonlinear AV methods have the same motivation as the corresponding ones in Example 1.

The numerical results corresponding to the three discretizations are summarized in Table 4.2. For different meshwidths ($h = 1/16$, $h = 1/32$, $h = 1/64$, $h = 1/128$), Table 4.2 presents the l^2-norm of the error away from the layers (denoted by $||\mathrm{E}||_{l^2}$), the l^2-norm of the undershoots (denoted by $||\mathrm{U}||_{l^2}$), and the l^2-norm of the overshoots (denoted by $||\mathrm{O}||_{l^2}$). The overshoots and undershoots are calculated the same way as in Example 1. The error away from the layers is calculated as the difference from 1 on the subdomain $y \geq x + 0.15$ and as the difference from 0 on the subdomain $y \leq x - 0.15$ and $0.15 \leq x \leq 0.9$.

The numerical results in Table 4.2 are consistent with the corresponding ones in Table 4.1. Indeed, the l^2-norm of the overshoots and the l^2-norm of the undershoots for the two nonlinear AV methods are consistently better than the corresponding errors for the SDFEM: as we refine the mesh, the l^2-norm of the overshoots is decreased by approximately three and four times. The l^2-norm of the error away from the layers is usually better for the two nonlinear AV methods as well, except for $h = 1/16$, when the mesh is too coarse, and $h = 1/128$. However, since we do not know the exact solution for our test problem, we can only make rough approximations of the error. Comparing the two nonlinear AV models, we see that the bounded AV model is consistently better.

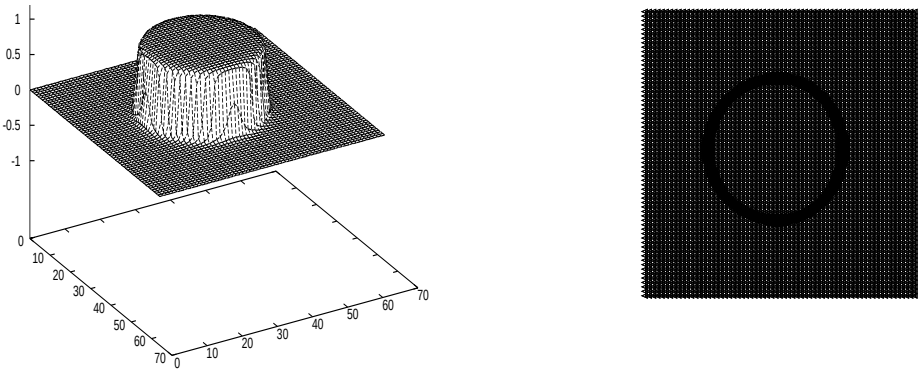

FIG. 4.1. *Example 1, the exact solution: surface plot and contour lines;* $h = 1/64$.

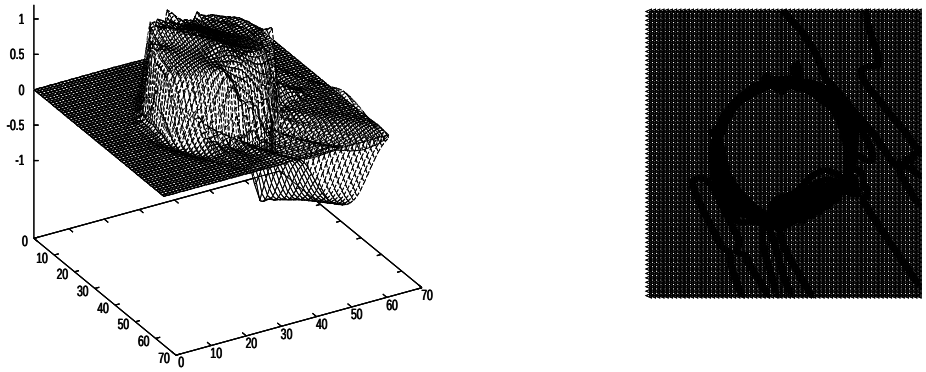

FIG. 4.2. *Example 1, the usual SDFEM method: surface plot and contour lines;* $\delta = h$, $h = 1/64$. *Note the poor solution quality (smearing, overshooting, and undershooting).*

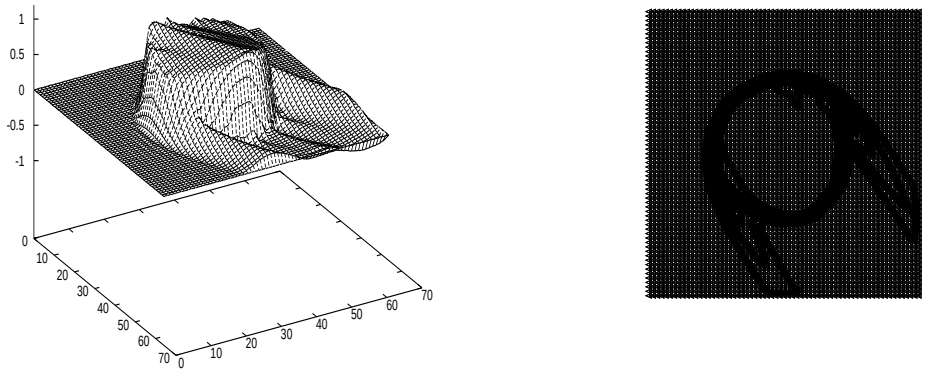

FIG. 4.3. *Example 1, the p-Laplacian AV SGS method: surface plot and contour lines;* $\mu = 10$, $\sigma = 1$, $p = 3$, $h = 1/64$. *Note the dramatic improvement in solution quality over Figure 4.2 (much smaller overshooting and undershooting).*

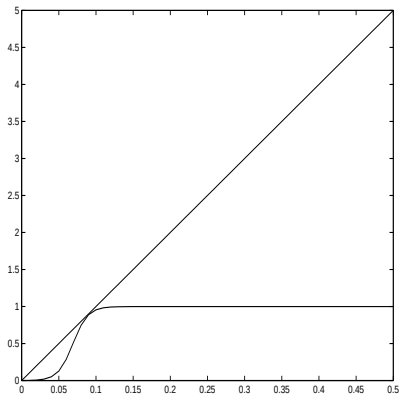

FIG. 4.4. *The graphs of* $a(|h\nabla u^h|)$ *and* $10 \cdot |h\nabla u^h|$*; the horizontal axis represents* $|h\nabla u^h|$.

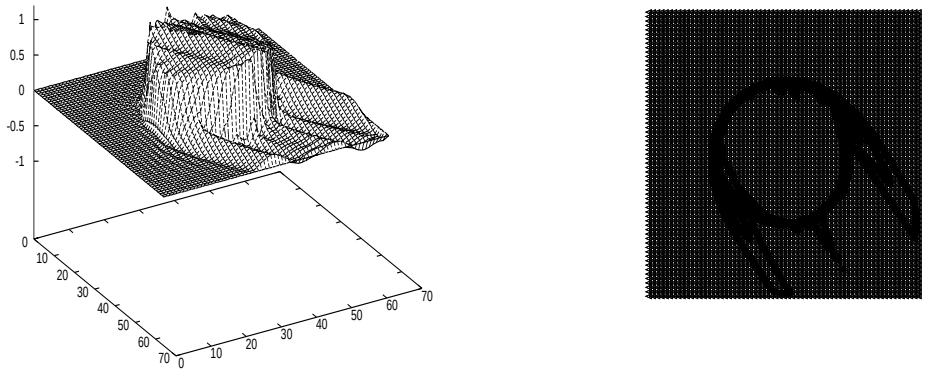

FIG. 4.5. *Example 1, the improved AV SGS method: surface plot and contour lines;* $\mu = 1$, $\sigma = 1$, $a(t) = -0.001 + 1/(1 + 999 \cdot e^{-100 \cdot t})$, $h = 1/64$. *Note the visible improvement over Figure 4.3 (sharper layer, less undershooting).*

TABLE 4.1
Example 1, norms of the errors for the three different discretizations. "E" represents the error, "U" represents the undershoots, and "O" represents the overshoots.

h	Norm	SDFEM	p-Laplacian AV	Bounded AV
1/16	$\|\|E\|\|_{L^2}$	.297+0	.328+0	.249+0
	$\|\|\|E\|\|\|$	.464+0	.496+0	.445+0
	$\|\|U\|\|_{l^2}$	.241+0	.164+0	.178+0
	$\|\|O\|\|_{l^2}$	.010+0	.000+0	.025+0
1/32	$\|\|E\|\|_{L^2}$	.231+0	.207+0	.161+0
	$\|\|\|E\|\|\|$	.359+0	.353+0	.337+0
	$\|\|U\|\|_{l^2}$	.142+0	.503-1	.664-1
	$\|\|O\|\|_{l^2}$	.391-2	.000+0	.993-2
1/64	$\|\|E\|\|_{L^2}$	.234+0	.126+0	.901-1
	$\|\|\|E\|\|\|$	.391+0	.375+0	.350+0
	$\|\|U\|\|_{l^2}$	.206+0	.354-1	.281-1
	$\|\|O\|\|_{l^2}$	.311-1	.194-1	.333-1
1/128	$\|\|E\|\|_{L^2}$	.225+0	.750-1	.511-1
	$\|\|\|E\|\|\|$	.329+0	.297+0	.265+0
	$\|\|U\|\|_{l^2}$	.206+0	.177-1	.144-1
	$\|\|O\|\|_{l^2}$	.472-3	.000+0	.560-3

TABLE 4.2
Example 2, norms of the errors for the three different discretizations. "E" represents the error away from the layers, "U" represents the undershoots, and "O" represents the overshoots.

h	Norm	SDFEM	p-Laplacian AV	Bounded AV
1/16	$\|\|E\|\|_{l^2}$	.117-1	.735-2	.138-1
	$\|\|U\|\|_{l^2}$	.269-1	.542-2	.126-1
	$\|\|O\|\|_{l^2}$	.787-2	.485-2	.576-2
1/32	$\|\|E\|\|_{l^2}$	.765-2	.368-2	.325-2
	$\|\|U\|\|_{l^2}$	.185-1	.139-1	.141-1
	$\|\|O\|\|_{l^2}$	.506-2	.199-2	.207-2
1/64	$\|\|E\|\|_{l^2}$	.171-2	.129-2	.100-2
	$\|\|U\|\|_{l^2}$	.444-2	.412-2	.374-2
	$\|\|O\|\|_{l^2}$	.174-2	.437-3	.434-3
1/128	$\|\|E\|\|_{l^2}$	.732-3	.883-3	.817-3
	$\|\|U\|\|_{l^2}$	.133-2	.964-3	.747-3
	$\|\|O\|\|_{l^2}$	.284-3	.551-4	.540-4

5. Conclusions. We presented two nonlinear AV models (a p-Laplacian AV model and a general, bounded AV model) for the numerical simulation of convection-dominated convection-diffusion problems. We started with a careful mathematical (existence, uniqueness) and numerical (a priori error estimates) analysis of the two models. Then, we tested these two models and the classical SDFEM method on two challenging problems with very sharp layers. The numerical results showed a dramatic improvement in solution quality for the two nonlinear AV models over the SDFEM. The best solution quality was obtained for the bounded nonlinear AV model. These results make the bounded nonlinear AV SGS model a promising approach for the numerical study of convection-dominated problems.

Acknowledgments. I thank Professor William J. Layton for generously bringing this problem to my attention, and for his help and constant support in writing this paper. I also thank Professor Daniel Ševčovič for his generous help in proving Lemma 3.2, and Professor Vince Ervin for helpful discussions that improved this paper.

REFERENCES

[1] J. Barrett and W. B. Liu, *Finite Element Approximation of the p-Laplacian*, Math. Comp., 61 (1993), pp. 523–538.
[2] J. Barrett and W. B. Liu, *Finite Element Approximation of Degenerate Quasilinear Elliptic and Parabolic Problems*, Numerical Analysis, D. F. Griffiths and G. A. Watson, Pitman Research Notes in Mathematics Series No. 303, Longman, 1994.
[3] M. Crouzeix and V. Thomée, *The Stability in L_p and W_p^1 of the L_2 Projection onto Finite Element Function Spaces*, Math. Comput., 48 (1987), pp. 521–532.
[4] Q. Du and M. Gunzburger, *Analysis of a Ladyzhenskaya Model for Incompressible Viscous Flow*, J. Math. Anal. Appl, 155 (1991), pp. 21–45.
[5] Q. Du and M. Gunzburger, *Finite Element Approximation for a Ladyzhenskaya Model for Stationary Incompressible Viscous Flows*, SIAM J. Numer. Anal., 27 (1990), pp. 1–19.
[6] K. Eriksson and C. Johnson, *Adaptive Streamline Diffusion Finite Element Methods for Stationary Convection-Diffusion Problems*, Math. Comput., 60 (1993), pp. 167–188.
[7] V. Girault and P. A. Raviart, *Finite Element Approximation of the Navier-Stokes Equations*, Springer-Verlag, Berlin, 1979.
[8] M. Gunzburger, *Finite Element Methods for Viscous Incompressible Flow: A Guide to Theory, Practice, and Algorithms*, Academic Press, Boston, 1989.
[9] T. J. R. Hughes and A. N. Brooks, *A Multidimensional Upwind Scheme with No Crosswind Diffusion*, AMD. ASME 34, New York, 1979.
[10] V. John, J. M. Maubach, and L. Tobiska, *Nonconforming Streamline-Diffusion-Finite-Element-Methods for Convection-Diffusion Problems*, Numer. Math., 78 (1997), pp. 156–188.
[11] W. J. Layton, *A Nonlinear, Subgridscale Model for Incompressible Viscous Flow Problems*, SIAM J. Sci. Comput., 17 (1996), pp. 347–357.
[12] W. J. Layton and B. Polman, *Oscillation Absorption Finite Element Methods for Convection-Diffusion Problems*, SIAM J. Sci. Comput., 17 (1996), pp. 1328–1346.
[13] J. L. Lions, *Quelques Méthodes de Résolution des Problèmes aux Limites Non Linéaires*, Dunod, Paris, 1969.
[14] J. M. Maubach, *Iterative Methods for Nonlinear Partial Differential Equations*, C.W.I. Press, Amsterdam, 1991.
[15] G. Minty, *Monotone (Nonlinear) Operators in Hilbert Space*, Duke Math. J., 29 (1962), pp. 341–346.
[16] B. Mohammadi and O. Pironneau, *Analysis of the K-Epsilon Turbulence Model*, John Wiley & Sons, Chichester, New York, Brisbane, Toronto, Singapore, 1994.
[17] U. Nävert, *A Finite Element Method for Convection-Diffusion Problems*, Ph.D. Thesis, Chalmers University of Technology, Göteborg, 1982.
[18] H. G. Roos, M. Stynes, and L. Tobiska, *Numerical Methods for Singularly Perturbed Differential Equations: Convection-Diffusion and Flow Problems*, Springer-Verlag, Berlin, 1996.
[19] J. Smagorinsky, *General Circulation Experiments with the Primitive Equation: I, The Basic Experiment*, Mon. Wea. Rev., 91 (1963), pp. 216–241.